Available online at www.sciencedirect.com
SCIENCE DIRECT®
Journal of Crystal Growth 287 (2006) 78–84
JOURNAL OF CRYSTAL GROWTH
www.elsevier.com/locate/jcrysgro

Effects of doping concentration and annealing temperature on properties of highly-oriented Al-doped ZnO films

Shou-Yi Kuo[a,*], Wei-Chun Chen[a,b], Fang-I Lai[c], Chin-Pao Cheng[b], Hao-Chung Kuo[d], Shing-Chung Wang[d], Wen-Feng Hsieh[d]

[a]*Instrument Technology Research Center, National Applied Research Laboratories, 20 R&D Road VI, Hsinchu Science Park, Hsinchu 300, Taiwan*
[b]*Department of Mechatronic Technology, National Taiwan Normal University, No. 162, Hoping E. Road, Section 1 Taipei 106, Taiwan*
[c]*Department of Electronic Engineering, Ching Yun University, 229 Jianshing Rd., Jungli City, Taoyuan 320, Taiwan*
[d]*Department of Photonics and Institute of Electro-Optical Engineering, National Chiao-Tung University, 1001 Ta Hsueh Road, Hsinchu 300, Taiwan*

Available online 1 December 2005

Abstract

Transparent and conductive high-preferential *c*-axis-oriented Al-doped zinc oxide (ZnO:Al, AZO) thin films have been prepared by the sol–gel route. Film deposition was performed by spin-coating technique on Si(1 0 0) and glass substrate. Structural, electrical and optical properties were performed by XRD, SEM, four-point probe, photoluminescence (PL) and UV-VIS spectrum measurements. The effects of annealing temperature and dopant concentration on the structural and optical properties are well discussed. It was found that both annealing temperature and doping concentration alter the microstructures of AZO films. Also, PL spectra show two main peaks centered at about 380 nm (UV) and 520 nm (green). The variation of UV-to-green band emission was greatly influenced by annealing temperatures and doping concentration. Reduction in intensity ratio of UV-to-green might possibly originate from the formation of Al–O bonds and localized Al-impurity states. The minimum sheet resistance of $10^4\,\Omega/\square$ was obtained for the film doped with 1.6 mol% Al, annealed at 750 °C. Meanwhile, all AZO films deposited on glass are very transparent, between 80% and 95% transmittance, within the visible wavelength region. These results imply that the doping concentration did not have significant influence on transparent properties, but improve the electrical conductivity and diversify emission features.

PACS: 70.; 73.61.Ga; 73.90+f; 68.60.−p

Keywords: B1. ZnO:Al; B2. semiconducting II–VI materials

1. Introduction

Zinc oxide (ZnO) is a wide-band gap II–VI semiconductor with very attractive properties such as high transparency in the 0.4–2 μm optical wavelength range, high piezoelectric constant, large electro-optic coefficient, and large exciton binding energy of ~60 meV at room temperature [1–4]. In recent years, the fabrication of ZnO-based films has attracted a considerable amount of interest due to their potential application in solar cells, gas sensors, optical waveguides, surface acoustic devices, piezoelectric transducers and varistors [5–9]. In addition, doping of ZnO with various elements has been reported to improve their electrical conductivity for use in optoelectric devices. Therefore, doped ZnO films are alternative materials to tin oxide and indium tin oxide, which have been widely used as transparent conducting oxide (TCO) because of their superior electrical and optical properties, abundance in nature, nontoxicity, and the excellent stability in hydrogen plasma, an unavoidable processing ambient in silicon-related fields [10].

It is well known that the structural properties and dopants may determine the electronic and photoluminescence (PL) properties of the materials. The typical dopants that have been used to enhance the conductivities of ZnO are the group III (B, Al, In, Ga) of the periodic table. Among them, Al-doped ZnO films have been widely

*Corresponding author. Tel.: +886 3 5779911; fax: +886 3 5773947.
E-mail address: u8624806@itrc.org.tw (S.-Y. Kuo).

0022-0248/$ - see front matter © 2005 Elsevier B.V. All rights reserved.
doi:10.1016/j.jcrysgro.2005.10.047

studied and are considered as candidate materials for organic electroluminescence displays [11]. Several techniques have been used for the preparation of ZnO thin films such as spray pyrolysis [12], chemical vapor deposition [13], sputtering [14], reactive evaporation [15], pulsed laser ablation, filtered cathodic vacuum arc technique [16,17], and hydrothermal method [18,19]. A number of reports have also been published on sol–gel-derived undoped and impurity-doped zinc oxide films [20–22]. Despite the crystalline quality being inferior to other vacuum deposition techniques, the sol–gel technique still has distinct advantages such as cost effectiveness, simplicity, excellent compositional control, homogeneity and lower crystallization temperature. Moreover, incorporation of dopants is easier in this technique. Hence, this technique is suitable for frontier researches.

In the present study, Al-doped ZnO (AZO) thin films with 0–5% molar concentrations were prepared by sol–gel method. Previous works mostly focused on the electrical and optical properties influenced by either dopants or thermal treatments. Different from their investigation, the influences of dopant concentration and thermal treatment on the structural, electrical and optical properties were investigated.

2. Experimental procedure

Zinc acetate-2-hydrate $[Zn(CH_3COO)_2 \cdot H_2O]$ and aluminum nitrate nonahydrate $[Al(NO_3)_3 \cdot 9H_2O]$ were chosen as the starting materials, and alcoholic solution were used as solvent. The details of the preparation method are similar to those described in earlier literatures. The concentration of zinc acetate was chosen to be $1\,mol\,l^{-1}$, and the precursor solution has been mixed thoroughly by a magnetic stirrer. Appropriate amounts of aluminum doping were achieved by adding aluminum nitrate to the precursor solution. In our experiment, the dopant level, determined by $100 \times [Al]/[Al+Zn]$, was varied from 0 to 5 mol%. The resultant solution was stirred at 80 °C for 2 h to yield a clear and homogeneous solution, which served as the coating solution after cooling down to room temperature. The coating was usually made 3 days after the solution was prepared.

The solution was spinning-coating onto fused quartz and Si(1 0 0) wafer substrates, which were rotated at 3000 rpm for 30 s. After each layer deposition, the gel layers were preheated at 350 °C for 20 min over a hot plate to evaporate the solvent and remove organic residuals. The process was repeated several times to obtain a desired thickness. After the deposition of the last layer, the films were inserted into a furnace and annealed in ambient atmosphere at several temperatures from 450–850 °C for 1 h.

X-ray diffraction (XRD, Siemens D5000) analyses were conducted using Cu-$K\alpha$ radiation to determine the crystallinity of the AZO films. Surface and cross-section morphology were examined by a Hitachi S-4300 scanning electron microscope (SEM). The electrical resistance was measured by a four-point probe method. Optical transmittance measurements were carried out using a UV–VIS–NIR spectrophotometer. The PL spectra were recorded at room temperature using a He–Cd laser at the wavelength of 325 nm as excitation source.

3. Results and discussions

Typical XRD patterns of the 3 mol% AZO thin films annealed at various temperatures are shown in Fig. 1(a). XRD spectra in Fig. 1(a) show that the sol–gel-derived ZnO:Al films developed without the formation of secondary phases and clusters such as Al_2O_3 and amorphous ZnO. All films exhibit only the (0 0 2) peak, indicating that they have *c*-axis preferred orientation due to self-texturing phenomenon. From Fig. 1(a), it is readily observed that the intensity of the (0 0 2) diffraction peak increases when the annealing

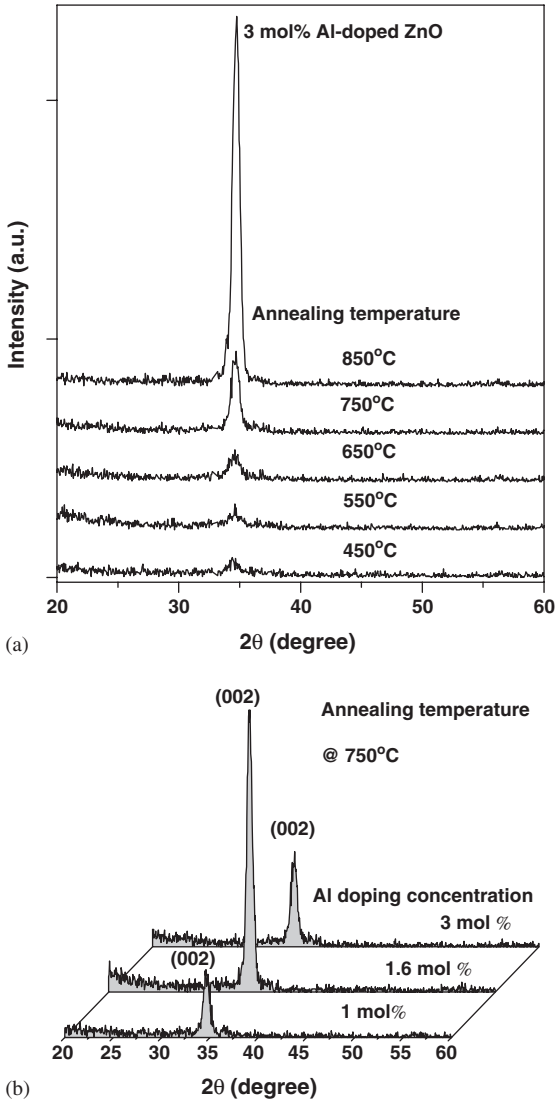

Fig. 1. (a) XRD patterns of 3 mol% Al-doped ZnO films as a function of the annealing temperature. (b) XRD patterns of 750 °C AZO films with 1, 1.6 and 3 mol% aluminum-doping concentration.

temperature rises up to 850 °C, and the crystallinity of the films determined from the full-width at half-maximum (FWHM) values shows the same trend. Both tendencies indicate a common representative of the improvement in crystalline quality with raising annealing temperature. Usually, it is suggested that the crystallinity can be enhanced while one increases the annealing temperatures, consistent with the XRD results of Fig. 1(a). To calculate the average grain size of the samples, the Scherrer's equation [23],

$$d = \frac{0.9\lambda}{B\cos\theta_B}, \quad (1)$$

is employed. Where λ is the x-ray wavelength of 1.54 Å, θ_B is Bragg diffraction angle, and B is the FWHM of θ_B. The calculated average crystallite sizes of pure ZnO thin films annealed at 450, 550, 650 and 750 °C are 10, 11, 11.5 and 13 nm, respectively. The results imply that the grain size of sol–gel-derived films enlarge with the increasing annealing temperatures, which can be understood by considering the merging process induced from thermal treatment. For ZnO nanoparticles, there are many dangling bonds related to the zinc of oxygen defects at the grain boundaries. As a result, these defects are favorable to the merging process to form larger grains while increasing the annealing temperature.

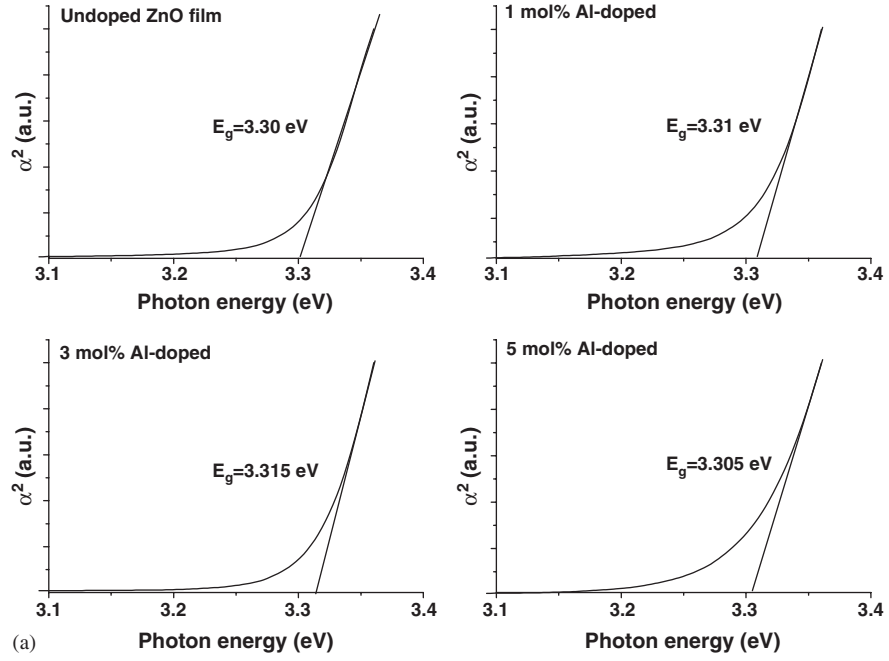

(a)

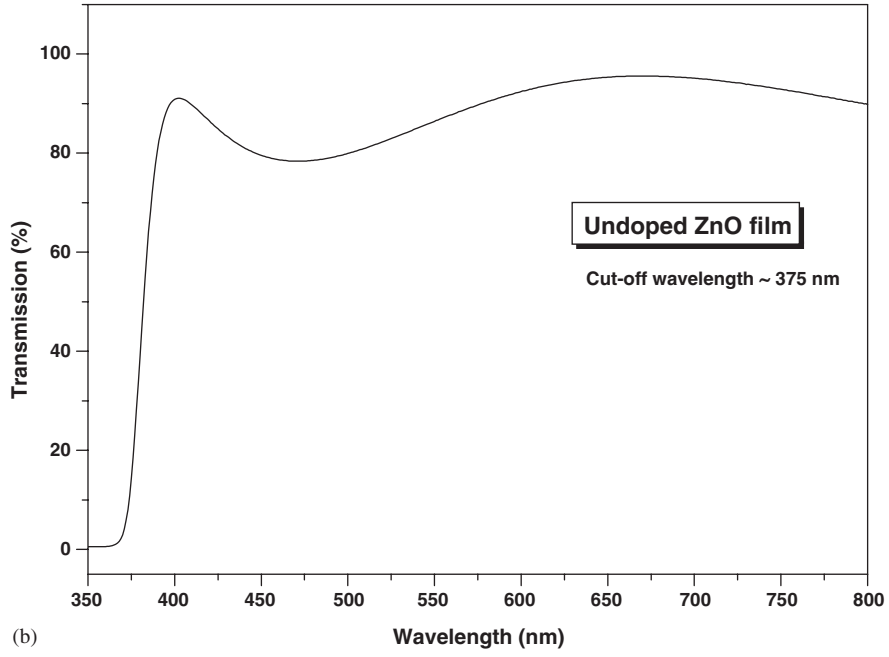

(b)

Fig. 2. (a) and (b) Plots of $(\alpha h\nu)^2$ against $h\nu$ for ZnO films with different Al-doping concentration, and the energy gap was obtained by extrapolating the linear absorption edge part. (b) The optical transmittance spectrum of undoped ZnO film annealed at 650 °C.

Moreover, the (0 0 2) diffraction peak intensities of AZO films decreased with increased doping concentrations more than 1.6 mol% as shown in Fig. 1(b). This indicates that an excess increase in doping concentration deteriorates the crystallinity of films, which may be due to the formation of stresses by the difference in ion size between zinc and the dopant and the segregation of dopants in grain boundaries for high doping concentrations.

As high transparency is the most important factor in the application of ZnO:Al films to TCOs, the optical transmittance was determined by a spectrophotometer within the wavelength from 350 to 850 nm. Regardless of the Al contents in the films, AZO films annealed above 450 °C demonstrate transmittance of above 80% in the range of the visible spectrum. Band gap energies estimated from the absorption edges of 750 °C annealed AZO films were shown in Fig. 2(a). Similar to the structure of ZnO, the ZnO:Al film has a direct band gap. The absorption edge for direct interband transition is given by [24]:

$$\alpha hv = C(hv - E_g)^{1/2}, \quad (2)$$

where C is a constant for a direct transition, and α is the optical absorption coefficient. The optical energy gap E_g can then be obtained from the intercept of $(\alpha hv)^2$ vs. hv for direct transitions. Better linearity for $(\alpha hv)^2$ vs. hv was observed as shown in Fig. 2(a), and the energy gap was obtained by extrapolating the linear absorption edge part of the curve using Eq. (2). Fig. 2(b) plots the transmittance of pure ZnO film. The sharp absorption edge revealed at wavelength of about 375 nm, which is very close to the intrinsic band gap of ZnO (3.3 eV), implies the films possess good crystal quality. It is noteworthy that a significant blue-shift in optical energy gap was examined while we raised the Al contents to 3 mol%. At the annealing temperature of 750 °C, the ZnO film doped with 3 mol% aluminum shows the largest optical band gap corresponding to the highest carrier concentration of the films. The observation might be due to the Burstein–Moss effect which described the blue-shifting of the absorption edge of a degenerate semiconductor with an increasing carrier concentration. On the other hand, the decrease of E_g for the ZnO films doped with 5 mol% Al suggests that excess Al atoms do not activate due to segregation at the grain boundaries.

Fig. 3 shows SEM micrographs of pure and 5 mol% AZO thin films annealed at various temperatures. The microstructure of the films consists of many round-shaped particles. With increasing annealing temperatures, the surface morphologies of the films reveal a noticeable transformation. At annealing temperature of 450 °C, the film contains fine grains and the particle size is about 50 and 20 nm for undoped and 5 mol% AZO films, respectively. Once annealing temperature increases, the grains become larger and densely packed. As expected, XRD analysis underestimates the mean grain size. Cracks are also observed in the films, and the formation of cracks probably originates from the different thermal expansion

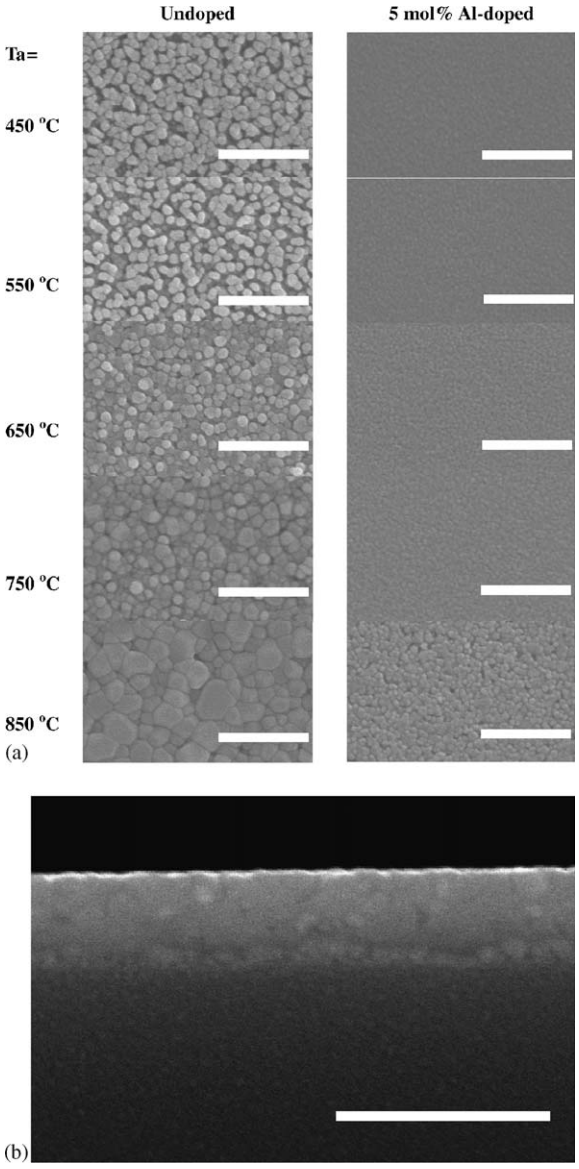

Fig. 3. (a) Planar SEM micrographs of undoped and 5 mol% Al-doped ZnO thin films annealed at various temperatures from 450 to 850 °C. (b) Cross-sectional SEM images of 5 mol% Al-doped ZnO film annealed at 750 °C, and the presence of two-layer can be observed. T_a represents the annealing temperature and the scale bar is 500 nm.

coefficients of the ZnO film and the substrate. In particular, the particle size of the films doped with aluminum became smaller with increasing doping concentration. This is because grain growth was disturbed by compression stresses due to the difference in ionic radii between zinc and aluminum ($r_{Zn^{2+}} = 0.074$ nm and $r_{Al^{3+}} = 0.054$ nm). Cross-sectional SEM image of 5% AZO thin film is shown in Fig. 3(b). The presence of two-layer can be observed from the SEM image, where grains near the substrate were round and a columnar structure was seen over the grains. During the nucleation process on lattice-mismatch substrates, a random orientation of the crystallites is obtained. Later, the crystallites are oriented with their fastest growth (0 0 1) planes during film growth, thus leading to axial

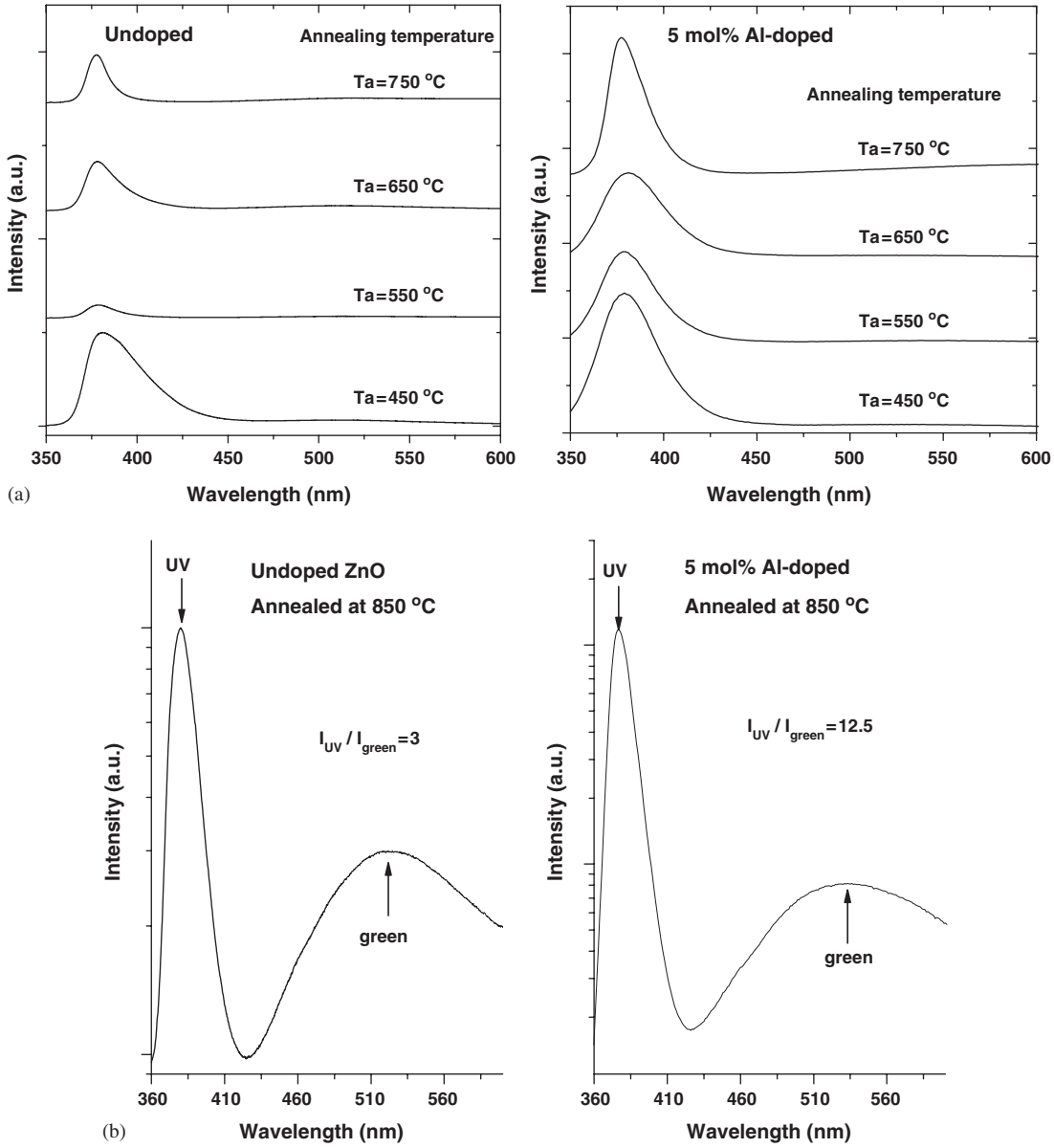

Fig. 4. (a) PL spectra of the undoped and 5 mol% Al-doped ZnO films annealed at various temperatures. (b) The UV-to-green emission ratio of 850 °C annealed undoped and 5 mol% Al-doped ZnO samples. The intense UV emission at 380 nm and the weak emission at approximate 520 nm, as indicated by arrows, are attributed to excitonic and defect-related recombination.

texture. Similar result has also been reported in other literature [25].

To investigate the effect of the annealing temperature on film quality, the room-temperature PL spectra of AZO thin films are plotted in Fig. 4. As shown in Fig. 4, the PL spectra of AZO show two distinct peaks: one narrow peak in the UV region and one broad green band. The UV emission centered at about 380 nm might originate from excitonic recombination corresponding to the band-edge emission. The defect-related green band is believed to relate to oxygen vacancies. It can be seen from Fig. 4 that the peak intensity of UV emission varies with annealing temperatures. In particular, all AZO films annealed at 450 °C shows the local maximum UV emission, and the UV emission intensity monotonically increases from 550 to 750 °C. Our observation is contrary to the common comprehension about the influence of thermal treatment on crystallinity. This behavior can be understood phenomenally by considering the formation of defects. As the ZnO film was annealed at low temperature of 450 °C, the rate of formation point defects is low. Accordingly, efficient excitonic emission can be easily achieved. For the temperature higher than 450 °C, more defects responsible for the nonradiative transition will be introduced into the films. This is why film annealed at around 550 °C show poor UV emission than that annealed at 450 °C. Furthermore, higher annealing temperatures (between 550–750 °C) facilitate the migration of grain boundaries and promote

the coalescence of small crystals, and thus favor a decrease of the concentration of nonradiative recombination centers. In addition to thermal treatment, dopant concentration plays an important role in the mechanism responsible for the luminescence as well. It is notable that the UV-to-green emission ratio decreases with increasing doping concentration. The intensity ratios of UV emission to green emission are 3 and 12.5 for the 850 °C annealed undoped and 5 mol% AZO films, respectively. One cause is most likely due to the formation of Al–O bonds in AZO films. It is known that the enthalpies of formation for Al_2O_3 ($\Delta G^0_{298} = -1492\,kJ/mol$) are much smaller than that for ZnO ($\Delta G^0_{298} = -324\,kJ/mol$). Thus the addition of Al dopants might prevent oxygen desorption from containing oxygen vacancies, which relates to the deep-level defects. This high intensity ratio manifests the addition of aluminum dopant modifies the intensity of green emission due to oxygen-deficient, which have been extensively discussed. Another possibility of the variation in intensity ratio can be ascribed to localized Al-impurity states [26]. The electron charge transfer from localized impurity states to the conducting states is reduced due to potential fluctuation of Al impurities formed in AZO films. We might speculate that an increase of localization energy due to high Al-doping induces an increase in nonradiative transition rate. Both probable mechanisms have contributed to the reduction in green-band emission. Further investigations are needed to verify the physical mechanism underlying.

Electrical resistivity variation of the films annealed at 750 °C as a function of doping concentration is plotted in Fig. 5. At 1.6 mol% aluminum doping, the lowest electrical resistivity values of film was obtained, which is approximately one order of magnitude smaller than others. It is well known that the n-type conductivity in non-stoichiometric ZnO is due to the presence of oxygen vacancies and interstitial zinc. Because the electrical conductivity of ZnO is directly related to the number of electrons, electrons formed by the ionization of the interstitial zinc and the oxygen vacancies will affect the electrical conductivity of ZnO. Comparing Al-doped with undoped ZnO films, the decrease in electrical resistivity at initial doping concentration might result from the increase in carrier concentration. However, the increase in the electrical resistivity with further increase in doping concentration may be due to a decrease in mobility of carriers caused by segregation of dopants at the grain boundary. In AZO films, aluminum was acting as an electrical dopant at initial doping concentration but as an impurity at higher doping concentrations. Also, the inset of Fig. 5 indicates that the electrical properties of AZO are modified by thermal treatments. Consequently, we can conclude that the doping concentration and thermal treatment are important factors in intrinsic and extrinsic defects of sol–gel-derived AZO films, and thus affects its electrical conductivity.

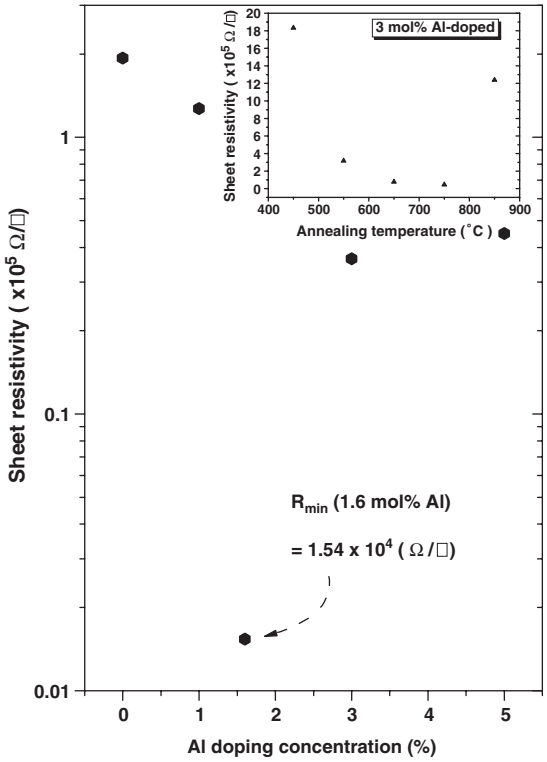

Fig. 5. Electrical resistivity variation of the films annealed at 750 °C as a function of Al-doping concentration. Also, the inset shows the sheet resistivity vs. annealing temperature of 3 mol% Al-doped ZnO films.

4. Conclusion

In conclusion, highly *c*-axis-oriented Al-doped ZnO thin films have been prepared by the well-established sol–gel technique under suitable thermal treatment. Structural, electrical, and optical properties were investigated to explore a possibility of producing TCO films through low-cost process. The impacts of the doping concentration and annealing temperatures on the structural and optical properties of the films were studied in detail. XRD results indicate that the crystallinity was enhanced as increasing annealing temperature. Meanwhile, the reduction in (0 0 2) diffraction peak reveals that an increase in doping concentration deteriorates the crystallinity quality, which may be due to the formation of stresses by the difference in ion size between zinc and the dopant and the segregation of dopants in grain boundaries. The evolution of grain size and texture due to aluminum dopant was characterized by SEM images. Particularly, the variation in UV emission intensity was attributed to the probability of formation of defects dominated by the annealing temperatures. In addition, dopant concentration also plays an important role in the mechanism responsible for the variation in intensity ratio of UV-to-green emission. The minimum sheet resistance of $1.54 \times 10^4\,\Omega/\square$ was obtained for the film doped with 1.6 mol% Al, annealed at 750 °C. These results indicate that suitable doping and thermal treatment cannot only improve the crystalline and electrical properties of AZO films, but also modify its luminescent characteristic.

Therefore, Al-doped ZnO films might be a promising candidate for further photonic applications.

References

[1] T. Minami, Mater. Res. Bull. 25 (2000) 38.
[2] Z. Jiwei, Z. Liangying, Y. Xi, Ceram. Int. 26 (2000) 883.
[3] C.C. Chang, Y.E. Chen, IEEE Trans. Ultrson. Ferroelectrics Freq. Control 44 (3) (1997) 624.
[4] D.L. Polla, R.S. Muller, R.M. White, IEEE Electron Device Lett. 7 (4) (1986) 254.
[5] J.A. Anna Selvan, H. Keppner, A. Shah, Mater. Res. Soc. Symp. Proc. 426 (1996) 497.
[6] V. Gupta, A. Mansingh, J. Appl. Phys. 80 (2) (1996) 1063.
[7] M. Bertolotti, M.V. Laschena, M. Rossi, A. Ferrari, L.S. Qian, F. Quaranta, A. Valentini, J. Mater. Res. 5 (9) (1990) 1929.
[8] K.-S. Weibenrieder, J. Muller, Thin Solid Films 300 (1997) 30.
[9] J.L. Deschanvres, B. Bochu, J.C. Joubert, J. Phys. 4 (3) (1993) 485.
[10] V. Fathollahi, M.M. Amini, Mater. Lett. 50 (2001) 235.
[11] J. Zhao, S. Xie, S. Han, Z. Yang, L. Ye, T. Yang, Synth. Met. 114 (2000) 251.
[12] R. Romero, M.C. Lopez, D. Leinen, F. Martin, J.R. Ramos-Barrado, Mater. Sci. Eng. B 110 (2004) 87.
[13] S. Fay, U. Kroll, C. Bucher, E. Vallat-Sauvain, A. Shah, Sol. Energy Mater. Sol. Cells 86 (2005) 385.
[14] J.C. Lee, K.H. Kang, S.K. Kim, K.H. Yoon, I.J. Park, J. Song, Sol. Energy Mater. Sol. Cells 64 (2000) 185.
[15] J.H. Morgan, D.E. Brodie, Can. J. Phys. 60 (1982) 1387.
[16] C. Yuen, S.Y. Yu, S.P. Lau, Rusli, T.P. Chen, Appl. Phys. Lett. 86 (2005) 241111.
[17] H.W. Lee, S.P. Lau, Y.G. Wang, K.Y. Tse, H.H. Hng, B.K. Tay, J. Crystal Growth 268 (2004) 596.
[18] F.K. Shan, Y.S. Yu, J. Eur. Ceram. Soc. 24 (2004) 1869.
[19] H. Nishizawa, K. Yuasa, J. Mater. Sci. Lett. 17 (1998) 985.
[20] Y.Q. Huang, M.D. Liu, Z. Li, Zhen, Y. Zeng, S.B. Liu, Mater. Sci. Eng. B 97 (2003) 111.
[21] S.Q. Chen, J. Zhang, X. Feng, X.H. Wang, L.Q. Luo, Y.L. Shi, Q.S. Xue, C. Wang, J.Z. Zhu, Z.Q. Zhu, Appl. Surf. Sci. 241 (2005) 384.
[22] Y. Natsume, H. Sakata, Thin solid films 372 (2000) 30.
[23] B.D. Cullity, Elements of X-ray Diffractions, Addison-Wesley, Reading, MA, 1978, p. 102.
[24] E. Ziegler, A. Heinrich, H. Oppermann, G. Stover, Phys. Stat. Sol. A 66 (1981) 635.
[25] I. Petrov, V. Orlinov, A. Misiuk, Thin Solid Films 120 (1984) 55.
[26] B.I. Shklovskii, A.L. Efros, Electronic Properties of Doped Semiconductors, Springer, New York, 1984.